

Primordial binary evolution and blue stragglers

Xuefei Chen^{1*} and Zhanwen Han¹

¹*National Astronomical Observatories/Yunnan Observatory, CAS, Kunming, 650011, P.R.China*

25 October 2018

ABSTRACT

Blue stragglers can significantly enhance the spectral energy toward short wavelengths, especially in ultraviolet and blue bands. Much evidence shows that blue stragglers are relevant to primordial binaries. In this paper, we systematically studied blue stragglers produced from primordial binary evolution via a binary population synthesis approach, and examined their contribution to the integrated spectral energy distributions of the host clusters. The mass transfer efficiency, β , is an important parameter for the final products (then blue stragglers) after mass transfer, and it is set to be 0.5 except for case A binary evolution. The study shows that primordial binary evolution may produce blue stragglers at any given times and that different evolutionary channels are corresponding for blue stragglers in different visual magnitude regions (in V band) on the colour-magnitude diagram (CMD) of clusters. The specific frequency of blue stragglers obtained from primordial binary evolution decreases with time first, and then increases again when the age is larger than 10Gyr, while that from angular momentum loss induced by magnetic braking in low-mass binaries increases with time and exceeds that of primordial binary evolution in a population older than 3 Gyr. Meanwhile, blue stragglers resulting from primordial binary evolution are dominant contributors to the ISEDs in ultraviolet and blue bands in a population between 0.3 and 2.0 Gyr. The value of β significantly affects on the final results, e.g the specific frequency of blue stragglers decreasing with β , blue stragglers produced from a high value of β being more massive, then contributing more to the ISEDs of the host clusters. For old open clusters, the assumption of $\beta = 1$ when the primary is in HG at the onset of mass transfer matches the observations better than that of $\beta = 0.5$ from the locations of BSs on the CMDs. Our study also shows that, for most Galactic open clusters, the specific frequency of blue stragglers obtained from our simulations is lower than that of observations, which is puzzling. Nevertheless, primordial binary evolution cannot account for *all* blue stragglers observed in old clusters.

Key words: binaries:close -stars:evolution - blue stragglers

1 INTRODUCTION

Blue stragglers (BSs) were first found by Sandage (1953). These stars have remained on the main sequence for a time exceeding that expected from standard stellar evolution theory. Many mechanisms, including single star models and binary models, have been presented to account for the existence of BSs (see the review of Stryker, 1993). At present, it is widely believed that more than one mechanism plays a role for the produce of BSs in one cluster and that binaries are important or dominant for the production of BSs in open clusters and in the field (Lanzoni et al. 2007; Dalessandro et al. 2008; Sollima et al. 2008). Binaries may produce BSs by way of mass transfer, coalescence of the two components, binary-binary collision and binary-single

star collision. The collision of binary-binary or binary-single may lead binaries to be tighter or farther apart. So a binary will advance or prolong mass transfer after collision, which may affect BS birth rate in a cluster. These collisions are relevant to dynamics and environment in the host cluster. Some works taking account of effects of collisions (Hurley et al. 2001; Hurley et al. 2005; Glebbeek, Pols & Hurley 2008) showed a significant importance of collisions for BS production in M67. However, in low density open clusters or in the field, the dynamical interaction should be small and have little contribution to BSs. In this paper, we are only concerned with BSs resulting from the evolutionary effect of primordial binaries, i.e. mass transfer and coalescence of two components.

Binary evolution has been well studied in the last 50 years, and it has been successfully used to explain many observed weird objects, such as Algols, Symbiotic

* xuefeichen717@hotmail.com

stars, cataclysmic variables, type Ia supernovae etc. Here we list some recent reviews on binary evolution and its application: van den Heuvel 2006, Webbink 2006, Bethe et al. 2007, Tutukov & Fedorova 2007, Langer & Petrovic 2008. In recent years, binary evolution has been applied in stellar population synthesis to study the characteristics of clusters and galaxies. For example, Han et al. (2007) provided a binary model for the UV-upturn of elliptical galaxies. Binaries differ from single stars in evolution due to mass transfer between the two components. The less massive component may accrete material from the more massive (or more evolved) one, and some strange phenomena appear as above in observations. Moreover, the two components may merge to become a single star. FK Com is believed to be a typical system which is in the final stage of coalescence (Stryker 1993). Binary mass transfer was originally advanced by McCrea (1964) to explain the BS phenomenon. A number of attempts have been made to test this hypothesis in open clusters ever since, from both detailed binary evolution and Monte Carlo simulations (Pols & Marinus 1994; Hurley et al. 2001; Hurley et al. 2005; Chen & Han 2004; Chen & Han 2008a; Chen & Han 2008b; Andronov et al. 2006; Tian et al. 2006). These studies show that primordial binary evolution (PBE), including mass transfer and coalescence of two components, are important for BS formation in some open clusters. However, these works are not enough to studying clusters from stellar population synthesis.

Recently, Xin and her collaborators (2005; 2007) investigated BSs in Galactic open clusters and examined their contributions to the integrated spectral energy distributions (ISEDs) of the host clusters. Their studies showed significant enhancements toward short wavelengths, especially in ultraviolet (UV) and blue bands. Their work provided a general picture of BSs in Galactic open clusters from observations. In this paper, we will systematically study the production of BSs from PBE using binary population synthesis and show their contribution to the host clusters in theory. Using this result, we may study the role of binary evolution of BS production in Galactic open clusters by way of comparing our results with observations.

We describe the binary population synthesis (BPS) model in section 2 and show the simulation results in section 3. In section 4, we selected some Galactic open clusters to compare with our calculations. The summary is shown in section 5.

2 EVOLUTIONARY CHANNELS AND THE BINARY POPULATION SYNTHESIS MODEL

2.1 Evolutionary Channels

According to the evolutionary state of the primary at the onset of mass transfer, three mass transfer cases are defined, i.e. case A for the primary being on the main sequence, case B for the primary after the main sequence but before central He burning, and case C for the primary during or after central He-burning (Kippenhahn & Weigert 1967). The secondary, as mentioned in section 1, may accrete material during Roche lobe overflow (RLOF) or merge

with the primary into a single star after RLOF. The mass ratio, $q = M_1/M_2$, of the two components at the onset of mass transfer is an important parameter in binary evolution. Here M_1 and M_2 are the masses of the mass donor and the accretor, respectively. If q is lower than a critical value, q_{crit} , the mass transfer is stable. The secondary goes upward along the main sequence in response to accretion, if it is a main sequence star, and becomes a BS when it is more massive than the turnoff of the host cluster (*Channel I*). All of the three cases above may produce BSs in this way but in various orbital period ranges (Chen & Han 2008b). It is also likely that the secondary fills its Roche lobe during RLOF and the system becomes a contact binary. Previous studies indicate that this contact binary will eventually coalesce as a single star (Webbink 1976; Eggleton 2000; Li, Han & Zhang 2005), although there are some controversies over the timescale of coalescence (Eggen & Iben 1989; van't Veer 1994; Dryomova & Svechnikov 2002; Bilir et al. 2005). If both components are on the main sequence, their remnant is also a main-sequence star (i.e. case A mass transfer) and evolves in a way similar to a normal star with that mass. So the remnant may be a BS if it is more massive than the turnoff (*Channel II*). If $q > q_{\text{crit}}$, mass transfer is dynamically unstable, and a common envelope (CE) is formed. The CE may be ejected if the orbital energy deposited in the envelope overcomes its binding energy, or the binary will merge into a single star. If the two components are main sequence stars, the remnant of coalescence will still be on the main sequence, and it is a BS if its mass is beyond the turn-off mass of the host cluster (*Channel III*). Binary coalescence of a contact binary or dynamically unstable RLOF (from case A mass transfer) is a popular hypothesis for single BSs (Mateo et al. 1990; Pols & Marinus 1994; Andronov et al. 2006; Chen & Han 2008a).

2.2 The binary population synthesis code

We employ the binary population synthesis code originally developed by Han et al. in 1994, which has been updated regularly ever since (Han, Podsiadlowski & Eggleton 1994; Han, Podsiadlowski & Eggleton 1995; Han et al. 1995; Han 1998; Han et al. 2002; Han et al. 2003; Han & Podsiadlowski 2004; Han, Podsiadlowski & Lynas-Gray 2007). With this code, millions of stars (including binaries) can be evolved simultaneously from the zero-main-sequence to the WD stage or a supernova explosion. The main input of the code is a grid of stellar evolution models, which are calculated from Eggleton's stellar evolution code (Eggleton 1971; Eggleton 1972; Eggleton 1973; Han, Podsiadlowski & Eggleton 1994; Pols et al. 1995; Pols et al. 1998). In this paper, we use a Population I model grid ($Z = 0.02$), including the evolution of normal stars in the range of $0.08 - 100.0M_{\odot}$ with hydrogen abundance $X = 0.7$ and helium abundance $Y = 0.28$ and helium stars in the range of $0.35 - 0.75M_{\odot}$. Single stars are evolved via interpolations in the model grid.

The main process for binary evolution we are concerned with is the first mass transfer as described in section 2.1. For this mass transfer, we adopt $q_{\text{crit}} = 3.2$ when the primary is on the main sequence or in the Hertzsprung gap. This value is supported by detailed binary evolution cal-

culations (Han, Tout & Eggleton 2000; Chen & Han 2002; Chen & Han 2003). If the mass donor is on the first giant branch or AGB, q_{crit} is obtained by setting $\zeta_{\text{S}} = \zeta_{\text{L}}$, where ζ_{S} and ζ_{L} are the adiabatic mass-radius exponent and Roche lobe mass-radius exponent of the mass donor (see Hjellming & Webbink (1987) for details), respectively, and they are fitted from the data of numerical calculations of Hjellming & Webbink (1987) and Soberman et al. (1997)(see also Han et al., 2001)(here after we use HW87 to present q_{crit} obtained from this way). Recently, some fully binary calculations (Han et al. 2002; Chen & Han 2008a) have demonstrated another expression of q_{crit} for mass transfer between a giant and a main sequence star. As an alternative, we also adopt the results of Chen & Han (2008b)(CH08 hereinafter) to examine the consequence of varying this value. The two descriptions of q_{crit} differ from each other. For instance, q_{crit} of HW87 results from a polytropic model and depends on the core mass fraction of the mass donor at the onset of RLOF and mass transfer efficiency during the RLOF, while that of CH08 is from detailed binary evolution calculation and depends on stellar radius, stellar mass and also on mass transfer efficiency. In CH08, the more evolved a star, the less stable the RLOF, while it is the opposite in HW87.

We assume that the mass transfer is always conservative for case A evolution, while 50 per cent of the matter from the primary is lost from the system for other cases. The mass lost from the system takes away a specific angular momentum in units of the specific angular momentum of the system (Podsiadlowski et al. 1992). We have not included angular momentum loss (AML) prior to RLOF. However, AML of low-mass binaries induced by magnetic braking is important for BS formation in old clusters. We examined its contribution to BSs in another way (see section 2.3) when the age is older than 1 Gyr.

The problem of the CE ejection criterion is still open at present. Here we introduce a classic α -formalism, including two model parameters, α_{CE} for the CE ejection efficiency and α_{th} for the thermal contribution to the binding energy of the envelope. The CE is ejected if

$$\alpha_{\text{CE}}\Delta E_{\text{orb}} > E_{\text{gr}} - \alpha_{\text{th}}E_{\text{th}}, \quad (1)$$

where ΔE_{orb} is the orbital energy released from orbital decay, E_{gr} is the gravitational binding energy and E_{th} is the thermal energy of the envelope. Both E_{gr} and E_{th} are obtained from full stellar structure calculations (Han, Podsiadlowski & Eggleton 1994; Dewi & Tauris 2000) instead of analytical approximations. We adopt $\alpha_{\text{CE}} = \alpha_{\text{th}} = 0.75$ or 1.0 in our model calculations¹.

In order to obtain the colours and the SED of the populations produced in our simulations, we use the latest version of the comprehensive BaSeL library of theoretical stellar spectra (Lejeune, Cuisinier & Buesel 1997; Lejeune, Cuisinier & Buesel 1998), which gives the colours

¹ As an alternative, Nelemans, Verbunt and Yungelson (2000) and Nelemans & Tout (2005) suggested a γ -algorithm from the view of the angular momentum balance to describe the CE evolution, which may explain the formation of all kinds of close binaries. However, as argued by Webbink (2007), *the significance of this finding is itself open to debate* (cf. Webbink, 2007).

and SEDs of stars with a wide range of metallicity Z , stellar surface gravity $\log g$ and effective temperature T_{eff} .

2.3 Angular Momentum Loss in Low-mass Binaries

The recent study of Chen & Han (2008a) demonstrated that AML is likely a main factor leading to BS formation in the old open cluster M67, indicating that AML should not be ignored in old clusters. We roughly estimated the AML contribution to BS formation in a similar way to Chen & Han (2008a). A semi-empirical formula for the orbital period variation is adopted here (Stepien 2006):

$$\frac{dP_{\text{orb}}}{dt} = -(2.6 + 1.3) \times 10^{-10} P_{\text{orb}}^{-1/3} e^{-0.2P_{\text{orb}}} \quad (2)$$

where P_{orb} is in days and time in years. For very short orbital periods the exponential factor is close to unity and varies very little during the subsequent evolution of the orbital period of the binaries, and consequently, it is ignored.

We will firstly find out the time, t_{RLOF} , at which the primary fills its Roche lobe for low-mass binaries. The Roche lobe of the primary R_{cr1} is calculated by (Eggleton 1983)

$$R_{\text{cr1}}/A = \frac{0.49q^{2/3}}{0.6q^{2/3} + \ln(1+q^{1/3})}, \quad (3)$$

where A is the separation and $q = M_1/M_2$.

The timescale from the onset of RLOF to being contact, and to the final coalescence are ignored here, since AML may lead the systems to reach contact, and then to coalesce very quickly (see Chen & Han, 2008a). Meanwhile, due to the very small evolution of the two components prior to RLOF, the remnants of coalescence are ZAMS stars with a total mass equal to the sum of the two components. If t_{RLOF} is less than the cluster age t_{c} , we then evolve the mergers to t_{c} and obtain the characteristics of the mergers at t_{c} .

2.4 Monte Carlo simulation parameters

To investigate BSs from mass transfer and binary coalescence, we performed a series of Monte Carlo simulations for a sample of 10^5 binaries (very wide binaries are actually single stars). A single starburst is assumed in the simulations, i.e. all the stars have the same age and metallicity ($Z = 0.02$). The initial mass function (IMF) of the primary, the initial mass ratio distribution and the distribution of initial orbital separation are as follows:

i) the IMF of Miller & Scalo (1979) is used and the primary mass is generated from the formula of Eggleton, Fitchett & Tout (1989):

$$M_1 = \frac{0.19X}{(1-X)^{0.75} + 0.032(1-X)^{1/4}} \quad (4)$$

where X is a random number uniformly distributed between 0 and 1. The mass ranges from 0.8 to $100M_{\odot}$.

ii) the mass ratio distribution is quite controversial. We include three different mass ratio distributions in the simulations. One is a constant distribution (Mazeh et al.1992) as

$$n(q') = 1, 0 \leq q' \leq 1 \quad (5)$$

where $q' = 1/q = M_2/M_1$. An alternative is a rising distribution

Table 1. Simulation sets (metallicity $Z = 0.02$) in this paper. $n(q')$ = initial mass ratio distribution; q_c = the critical mass ratio with the first RLOF in FGB or AGB; α_{CE} = CE ejection efficiency; α_{th} = thermal contribution to CE ejection.

Set	$n(q')$	q_c	α_{CE}	α_{th}
1	constant	HW87	0.75	0.75
2	Uncorrelated	HW87	0.75	0.75
3	Rising	HW87	0.75	0.75
4	constant	CH08	0.75	0.75
5	constant	HW87	1.0	1.0

$$n(q') = 2q', 0 \leq q' \leq 1 \quad (6)$$

or the third case where both components are chosen randomly and independently from the same IMF (uncorrelated).

iii) We assume that all stars are members of binary systems and the distribution of separations is constant in $\log a$ (a is separation).

$$an(a) = \begin{cases} \alpha_{sep}(a/a_0)^m, & a \leq a_0 \\ \alpha_{sep}, & a_0 < a < a_1 \end{cases} \quad (7)$$

where $\alpha = 0.070$, $a_0 = 10R_\odot$, $a_1 = 5.75 \times 10^6 R_\odot = 0.13\text{pc}$ and $m = 1.2$. This distribution gives an equal number of wide binary systems per logarithmic interval and 50 per cent of systems are with orbital periods less than 100 yr (Han, Podsiadlowski & Eggleton 1995).

3 SIMULATION RESULTS

We performed five sets of simulations (see Table 1) for a Population I composition ($X = 0.70$, $Y = 0.28$ and $Z = 0.02$) to systematically investigate the BS formation from PBE. The age ranges from 0.1 to 20 Gyr. The first set is a standard set with the best choice model parameters from the study of the formation of hot subdwarfs (Han et al. 2002, 2003). We vary the model parameters in the other sets to examine their influences on the final results².

From our simulation, PBE may produce BSs at any given time. For the standard set, we plotted colour-magnitude diagrams (CMDs) such as Fig. 1 of the population at all ages we studied and obtained some whole properties of BSs from PBE. Due to the size limit of this paper, we have not shown other CMDs here and just describe some whole properties as follows. One may send a request to xuefeichen717@hotmail.com for these figures.

3.1 Distribution on colour-magnitude diagrams

Fig. 2 shows the distributions of BSs around the turnoff at various ages from both mass transfer (*Channel I*, the dotted lines) and binary coalescence (*Channels II and III*, the solid lines). The abscissa is magnitude difference between BSs and

the turnoff, that is, $\Delta M = M_{BS} - M_{to}$, where M_{BS} and M_{to} are the bolometric (or visual) magnitudes of the BS and of the turnoff, respectively. Two sets of magnitude difference (bolometric and visual) are presented in this figure to show the difference between the intrinsic and observed. Due to high bolometric corrections for massive stars, BSs move toward high-magnitude regions in comparison to the turnoff after bolometric correction when the population is younger than 1Gyr.

From Figs. 1 and 2 we see that, many BSs are below but bluer than the turnoff. They may extend into the region 1 mag (hereinafter mag or magnitude means visual magnitude without expression) lower than the turnoff. These objects are mainly from *Channels I and III*. They are less evolved than the turnoff and may contribute more to the flux of V band in the following evolutions. Most BSs from *Channels I and III* are within 1.5 mag of the turnoff, while some ones from *Channel II* may have magnitudes lower than the turnoff by about 2.3 mag. For *Channels I and III*, the secondaries either accrete only a part of the primary's mass or have very low initial masses (because of large q), while the secondaries undergoing *Channel II* have relatively high initial masses and the sum mass of two components is conserved for the remnants. Thus, BSs from *Channel II* are generally more massive than those from *Channels I and III*. However, *Channel II* cannot produce BSs 3 mag brighter than the turnoff. Extremely high luminous BSs have been observed in some open clusters, e.g F81 in old open cluster M67. It is believed that F81 is likely from triple (or more) stars. Whatever, PBE without dynamical interaction cannot account for *all* BSs even in open clusters.

Between 0.4 and 1.5 Gyr, BSs with high magnitudes (i.e very close to the turnoff) scatter all over the main sequence and the spread decreases with increasing mass. This phenomenon gradually disappears with time, and eventually, the spread of BSs on the main sequence is similar for various masses. The time scales of BSs in different magnitude regions at various ages can account for this. For BSs near the turnoff, they have relatively longer main-sequence time scales than those further away from the turnoff, especially when the population is young. Thus, some BSs near the turnoff are likely very close to zero-age main sequence and some BSs formed earlier move to the red side of the main sequence, resulting in a large spread around the turnoff. However, it is different for massive BSs. Since the population is young, massive BSs have very short main-sequence timescales and so is unlikely to stay close to the zero-age main sequence, leaving gaps in these regions. With increasing age, BSs with relatively high mass are also likely to be close to the ZAMS, and then the scatter is similar for BSs with various masses.

The effect of contact binaries (*Channel II*) on BSs is intermittence. For example, BSs formed in this way appear at one time and disappear for the following time (i.e. the earlier BSs evolve off the main sequence while no new BSs are produced), and then appear again later. The intermittence comes from the very short time scales for the BSs formed in this way. Due to the relatively high mass, BSs from this way (if they exist) are main contributors to the ISED of the host clusters. As we compare our results with M67, some observed BSs are obviously located in the region from this channel (see Fig. 1), indicating *Channel II* having an effect

² Note that AML has not been included in any of the five sets. The contributions of AML are calculated separately from PBE by the method of section 2.3.

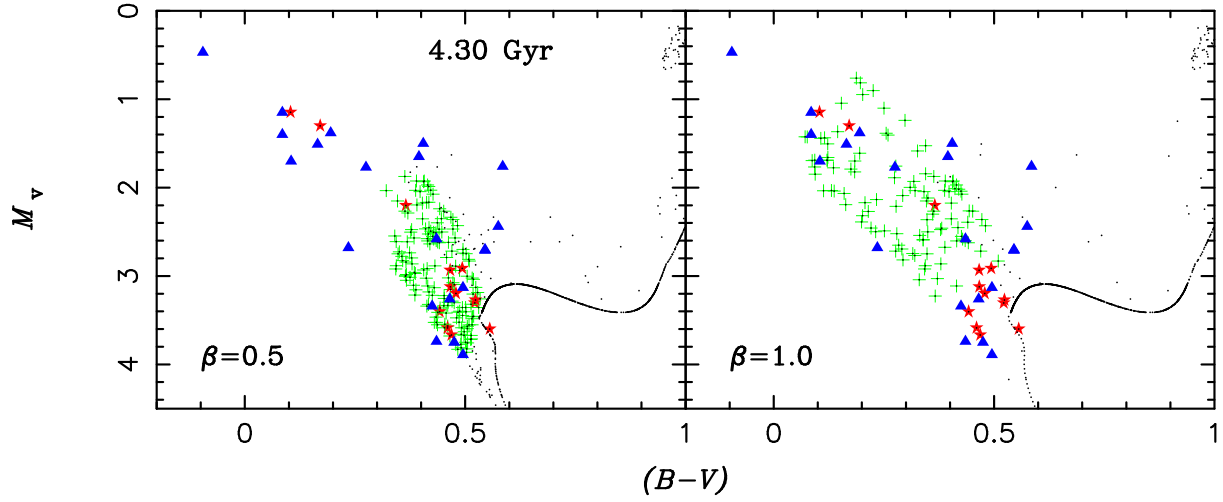


Figure 1. Colour-magnitude diagrams when the population is at 4.3Gyr. Here β is the mass fraction of the matter lost from the primary accreted by the secondary when the primary is in HG at the onset of RLOF. The green crosses and red stars are for BSs from mass transfer and binary coalescence, respectively, and the small black dots are for other objects in the population. The triangles are observed BSs of M67 from Sandquist et al. (2003).

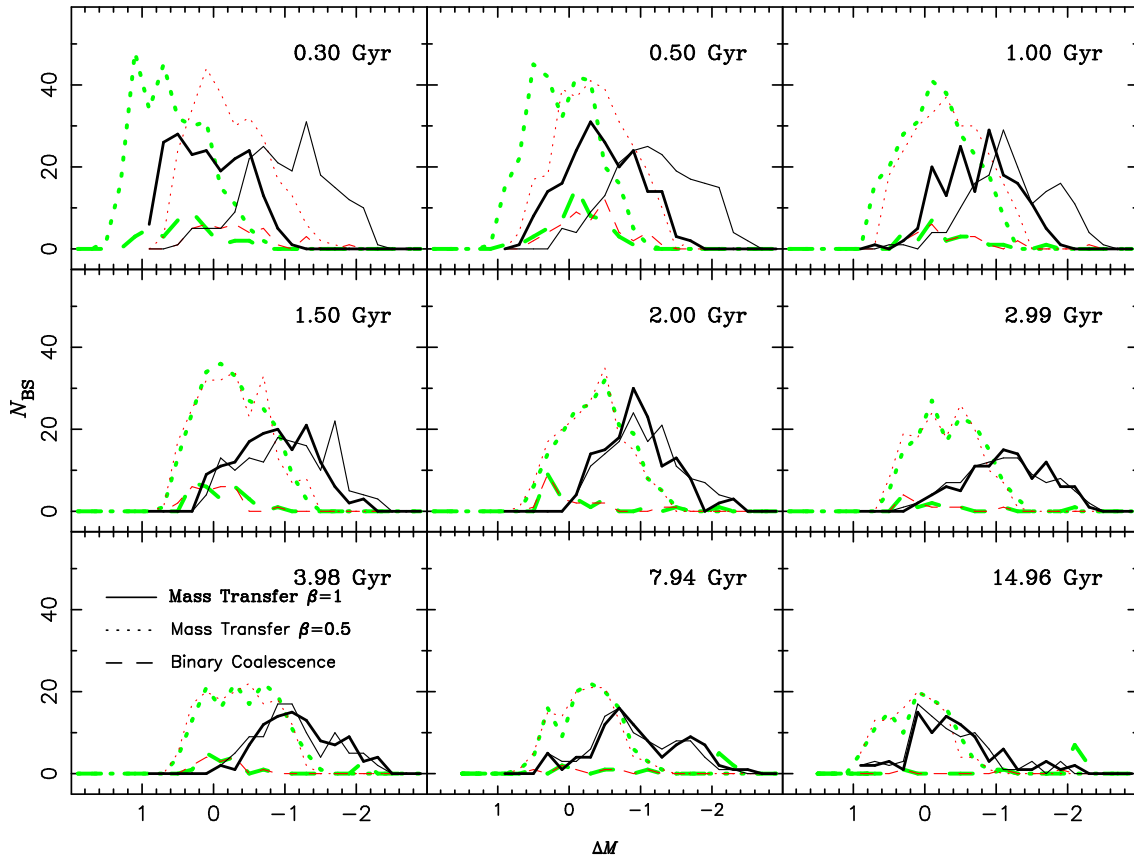


Figure 2. Distribution of BSs around the turnoff from primordial binary evolution for different channels (i.e. mass transfer and binary coalescence). The abscissa is magnitude difference between BSs and the turnoff. The thick lines are for visual magnitude (i.e. after bolometric corrections) and the thin ones are for bolometric magnitude. Note that BSs from AML are not shown in this figure.

on BS formation in this cluster, although the effect might be small.

3.2 The Specific Frequency

The BS number from the simulations, N_{BS}^{b} , depends slightly on the population age in our simulations, while the specific frequency, $\log F_{\text{BSS}} (\equiv \log(N_{\text{BS}}^{\text{b}}/N_2^{\text{b}})$, N_2^{b} is the number of stars within 2 mag below the main-sequence turnoff), heavily depends on the age due to the increase of N_2^{b} , as shown in Fig. 3, which includes the results from different calculation sets (the upper panel, no AML having been included) and from different evolutionary channels in the standard simulation set (set 1, the bottom panel).

From Fig. 3 we see that, in all of the five sets, $\log F_{\text{BSS}}$ decreases with time first, and then increases when the age, t , is larger than 10 Gyr. The decrease of $\log F_{\text{BSS}}$ before 1.5 Gyr comes from the increase of N_2^{b} . After that, the number of potential binaries which may contribute to BSs decreases, leading to fewer BSs formed. On the other hand, N_2^{b} continues increasing. Thus, $\log F_{\text{BSS}}$ continues decreasing. With increasing time, the primaries in long-orbital-period binaries gradually enter into AGB phase, dramatically expand, and some of them may fill their Roche lobe and start RLOF. Due to large stellar winds in the AGB phase, these mass donors at the onset of RLOF are probably much less massive than before and this mass transfer is easily stabilized, resulting in some long-orbital-period BSs. In the standard set, the long-orbital-period BSs first appear at 2.24 Gyr, and increase in number with time, since more primordial binaries with long-orbital periods become contributors to BS numbers with time. As a consequence, $\log F_{\text{BSS}}$ begins to increase when $\log(t/\text{yr}) > 10$.

As shown in Fig. 3, the distribution of the initial mass ratio is the main factor affecting the BS specific frequency, since both the onset time and the stability of RLOF are relevant to initial mass ratios. The value of $\log F_{\text{BSS}}$ depends slightly on the critical mass ratio for dynamically stable RLOF, especially when $\log(t/\text{yr}) > 9.2$, when binaries with long-orbital periods start contributing to BS formation. Both α_{CE} and α_{th} have hardly any effect on $\log F_{\text{BSS}}$, since BSs from binary coalescence (not including AML) are always much fewer than those from mass transfer during the whole age (see the bottom panel of this figure).

The contribution from AML when $\log(t/\text{yr}) > 9$ is also presented in the bottom panel of Fig. 3. We see that AML becomes more and more important for BS formation with time, since more and more low-mass binaries are close enough to start RLOF with time due to AML. The contribution from AML exceeds that from primordial binary evolution when $\log(t/\text{yr}) > 9.4$. Thus, AML in low-mass binaries should not be ignored when we study BSs from binaries in old clusters.

3.3 Contribution to ISED

To demonstrate the contribution of BSs from PBE to ISEDs, we plotted ISEDs of a population for various cases in Fig. 4, where SSP means a population without binary interaction. This figure shows that BSs resulting from binary evolution are dominant contributors to the ISED in UV and

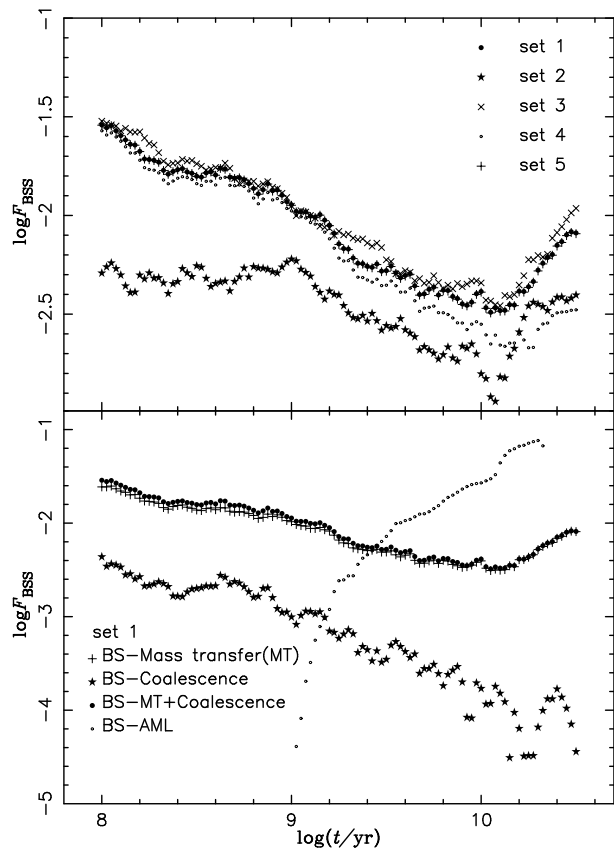


Figure 3. Specific frequency of BSs from primordial binary evolution for different simulation sets (the upper panel, without AML) and for different channels in the standard simulation set (set 1, the bottom panel). The result of set 2 is obviously different from the others since we adopted an *uncorrelated* initial mass ratio distribution.

blue bands between 0.3 and 2.0 Gyr. The BSs and SSP have comparable energy in UV and blue bands between 2 and 4 Gyr. The contribution from AML becomes more important with time, and exceeds that from primordial binary evolution for a population older than ~ 3 Gyr. Thus, primordial binaries are important contributors to BSs over the whole age range.

In most cases, binary coalescence is much less important than mass transfer, as shown in Fig. 4. However, binary coalescence may produce BSs with high masses, which then have lower magnitudes i.e they may be about 2.5 magnitude brighter than the turnoff (see Figs. 1 and 2). Once these massive BSs are produced, they become the dominant contributors to the ISEDs in the UV, even if there is only one.

3.4 Influences of the mass transfer efficiency

The mass transfer efficiency, β , is defined as the mass fraction of the matter lost from the primary accreted by the secondary. In the above study, β is set to be 0.5 except for case A binary evolution. In fact, this value is unclear at present. It might be higher when the mass donor is in HG, while lower when the mass donor is on FGB or AGB. What is the result if we change this value, e.g $\beta = 1$ when the primary is in HG at the onset of RLOF?

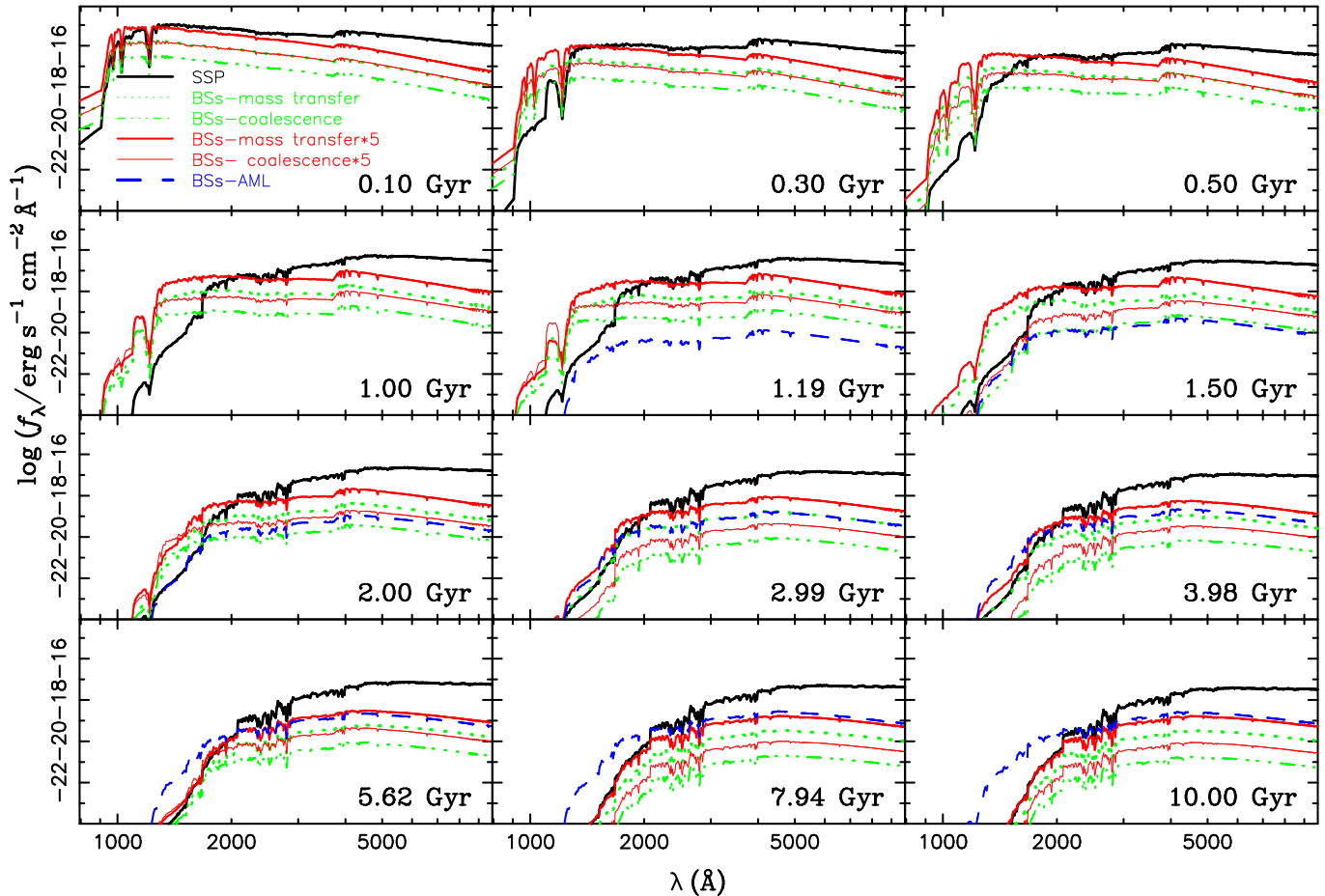


Figure 4. Integrated rest-frame intrinsic SEDs for a stellar population (including binaries) with a mass of $1M_{\odot}$ at a distance of 10kpc for set 1 with $\beta = 1$ when the primary is in HG at the onset of RLOF. The black solid lines are for the results of SSP, which means a population without binary interaction, and the others are the contributions of BSs from different evolutionary channels. Note that the red solid lines are 5 times contributions of BSs from mass transfer (the thick ones) and from binary coalescence (the thin ones). We see that BSs resulting from PBE (without AML) are dominant contributors to the ISED in UV and blue bands between 0.3 and 2.0 Gyr. The BSs and SSP have comparable energy in UV and blue bands between 2 and 4 Gyr. The contribution from AML becomes more important with time and exceeds that from primordial binary evolution when the population is older than 3 Gyr.

Obviously, the secondary may accrete more material from the primary, and then is more likely to become a BS. From this view, it seems that we may obtain more BSs when $\beta = 1$. However here we ignored another important fact, that is, the lifetime of the secondary on the main sequence after RLOF. We now consider a simple case: the turnoff of a cluster $M_{\text{to}} = 1M_{\odot}$, and $q_c = 3.2$ when the mass donor is on the MS and in HG. In this case, the initial mass of the secondary M_{2i} should be less than $1M_{\odot}$ to ensure the secondary to become a BS, and binaries with M_{1i} less than $3.2M_{\odot}$ possibly contribute to BSs via stable RLOF. We firstly see the result of binaries with the primary having initial mass of $M_{1i} = 1.6M_{\odot}$, the final mass of which is approximately assumed to be $0.6M_{\odot}$. This assumption is appropriate according to the initial-final mass relation of Han, Podsiadlowski & Eggleton (1994). The primary then lost $1M_{\odot}$ during RLOF. The minimum mass of the secondary for stable RLOF is $M_{2i}^{\text{min}} = 1.6/3.2 = 0.5M_{\odot}$. As a consequence, the secondary mass would range from 1 to $1.5M_{\odot}$ for $\beta = 0.5$, and from 1.5 to $2M_{\odot}$ for $\beta = 1$ after RLOF. This means that all the possible BSs from binaries with $M_{1i} = 1.6M_{\odot}$ (via stable

RLOF) have already been counted when $\beta = 0.5$. When we adopted $\beta = 1$, we only increased the masses of the products while not the number. As well, the products from $\beta = 1$ have much less lifetimes on the main sequence in comparison to those from $\beta = 0.5$. Thus, after some time, the number of BSs from binaries with $M_{1i} = 1.6M_{\odot}$ when $\beta = 1$ will be less than that of $\beta = 0.5$. The binaries with M_{1i} between 1.6 and $3.2M_{\odot}$ have similar results like this. Another case is that, when $\beta = 0.5$, some secondaries cannot increase their masses to become BSs while can when $\beta = 1$ (i.e. $M_{1i} < 1.6M_{\odot}$), leading to an increase of the BS number. In this case, if $\beta = 1$, the original BSs from $\beta = 0.5$ will be more massive and have shorter lifetimes on the main sequence. The final number of BSs is related to the completion of the two facts. We examined set 1 with $\beta = 1$ and found that the BS number decreased while N_2 increased in comparison to those of $\beta = 0.5$. The specific frequency of BSs when $\beta = 1$ is then smaller than that of $\beta = 0.5$.

However it should be noticed that BSs from $\beta = 1$ may be more massive than those of $\beta = 0.5$, which may explain some BSs with far away from the turnoff (see the right panel

of Fig.1), especially, we may obtain BSs with masses larger than 2 times of the turnoff even these objects have very short lifetimes. For old clusters, since the binaries contributing to BSs are less massive than those in young clusters, it is then appropriate to assume a high value of β . We will see in section 4 that the assumption of $\beta = 1$ matches the observations better than that of $\beta = 0.5$ for King 2, NGC 188, IC 1369 and NGC 2682. Since BSs from a high β have higher masses, their contributions to ISED then become more important in ultraviolet and blue bands. Fig.5 shows the ISEDs for the same population as that in Fig.4 but $\beta = 1$ when the primary is in HG at the onset of RLOF. We found that the value of β significantly affects the BS contribution to ISEDs, that is, a large β results in more contribution in ultraviolet and blue bands. When $\beta = 1$, BSs from PBE dominate the ISEDs in ultraviolet and blue bands till 5.6Gyr, after which their contributions become smaller than those of BSs from AML.

Correspondingly, the distribution of BSs from stable mass transfer is changed at different values of β . The results of $\beta = 1$ are plotted in Fig.2, from which we see that more BSs with lower magnitudes (or brighter than the turnoff) are obtained at this value.

4 THE ROLE OF PBE FOR PRODUCING BSS IN GALACTIC OPEN CLUSTERS

We select some Galactic open clusters with metallicities similar to that of the Sun (i.e. around 0.02) to examine BSs from primordial binary evolution. Table 2 shows the characteristics of these clusters and their BS information from both observations and our simulations.

In the new BS catalogue of Ahumada & Lapasset (2007) (hereafter AL07), the authors showed a schematic diagram for the regions of BSs on a colour-magnitude diagram to identify BSs. They have not given a definitive area for BSs on a CMD. In this paper, we simply define BSs as main sequence stars which have masses larger than the turnoff mass of the host clusters. We will see later that BSs defined in this way are well matched with the region defined in AL07.

To demonstrate the importance of PBE for BS formation in a cluster, we introduce a factor, f , which is defined as:

$$f = N_{bs}^b / N_2^b \cdot N_2 / N_{bs}, \quad (8)$$

where N_{bs}^b and N_2^b are the numbers of BSs and stars within a 2 mag interval below the main-sequence turnoff point of the host cluster from the simulations, respectively, and N_{bs} and N_2 are from observations. Thus, f is actually the ratio of the BS number expected from PBE to that observed. The values of f from different calculations are also presented in Table 2.

Figs. 6 to 11 present colour-magnitude diagrams for the sample clusters in Table 2 (the clusters appear in the same order as that in Table 2 in these figures), where the crosses are BSs from PBE and the squares are observed BSs. We have not shown the clusters for which no BSs were presented in AL07.

4.1 Discussions on the sample clusters

From Figs.6 to 11 we see that some observed BSs are in the appropriate regions obtained from PBE, while some are not. The outlying BSs may be divided into four cases as follows³.

(i) Some observed BSs are much more luminous in the V band than the turnoffs of the host clusters, such as, in IC 1369, IC 4756, King 2, NGC 188, NGC 2287, NGC 2682, NGC 6067 and NGC 6416. These luminous BSs are likely from *Channel II* except for the most luminous BS in NGC 2682 (F81), but this channel seems to have an effect only in King 2 from the CMDs of these clusters. We know that *Channel II* is very sensitive to the cluster age (see Section 3.1), but the age determination of a cluster is very uncertain at present. For instance, the age of NGC 2682 may range from 3 (Bonatto & Bica 2003) to 6 Gyr (Janes & Phelps 1994). Thus, it is still possible that *Channel II* leads to the production of these luminous BSs. Another possibility is that the mass fraction of the matter lost from the primary and accreted by the secondary (β) is more than 50 per cent when the primary is in HG. Obviously, we may obtain more luminous objects with a high β . As mentioned in section 3.4, it is appropriate to assume a high value of β in old clusters. We re-plotted CMDs with $\beta = 1$ for clusters King 2, NGC 188, IC 1369 and NGC 2682 in Fig.12, from which we see that the assumption of $\beta = 1$ matches the observations better than that of $\beta = 0.5$ for the four clusters.

(ii) Some BSs are redder than those obtained from PBE, such as in IC 166, IC 1311, IC 2488, Melotte 105, NGC 2437 and NGC 6940 (also in King 2, NGC 188 and NGC 2682). These objects are likely sub-giant stars from their locations on the CMDs. Thus, they are ruled out by the BS definition (only stars on the main sequence are included) in this paper.

(iii) Several BSs from AL07 are below the turnoffs, but bluer than normal stars on the main sequence with the same masses⁴, such as in IC 1311, Melotte 105, Melotte 111, NGC 2539, NGC 2660, NGC 2818, NGC 3532 and NGC 6939. These objects are inside the region defined in AL07, but have masses lower than the turnoffs, thus, they are also ruled out by the BS definition in this paper.

(iv) Several observed BSs are bluer than those from PBE, such as in IC 4756, NGC 188, NGC 3114 and NGC 3496. Enhancement of surface helium abundance of BSs from *Channels I and II* may lead them to be bluer than those shown in the figures, but the blueshift is within 0.1 mag, as shown in Chen & Han (2004; 2008a). BSs which are bluer beyond 0.1 mag than the left side of the region from PBE (i.e in IC 4756) could have larger He abundances than the examples shown in Chen & Han (2004; 2008a). AGB stars can provide material with high He abundances, but from the simulations this only occurs in populations older than 2.24 Gyr for Population I. Thus, it is possible that these BSs

³ Note that even though the BSs locate in the appropriate regions, it is also possible to produce them in other ways. For instance, BSs from AML are also around the turnoff of the cluster (Chen & Han 2008a).

⁴ Here 'normal' means that the stars have not passed through RLOF, during which a low-mass main sequence star may increase its mass by accretion. After RLOF, the accretor is rejuvenated and bluer than a normal star with the same mass.

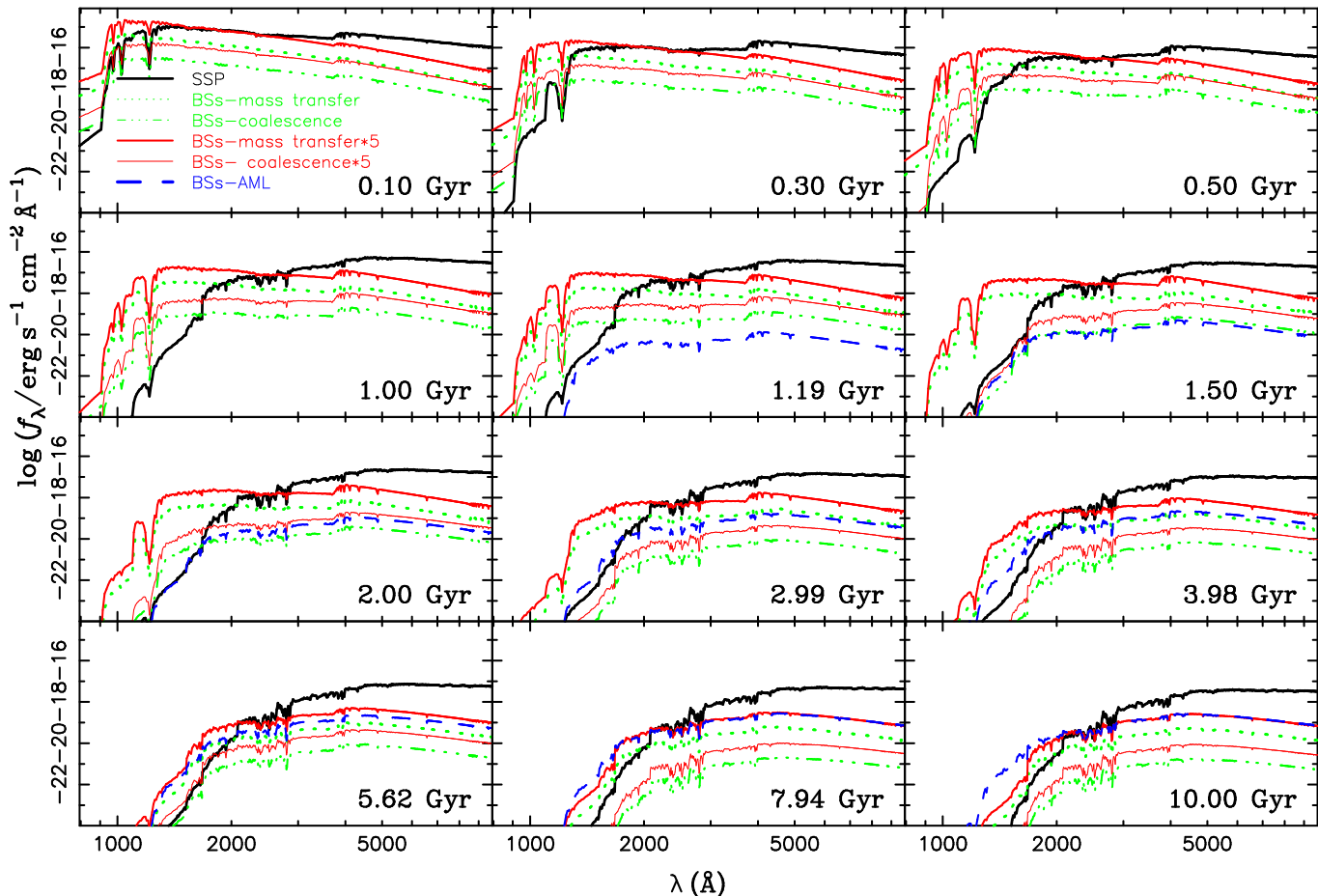


Figure 5. Integrated rest-frame intrinsic SEDs for a stellar population (including binaries) with a mass of $1M_{\odot}$ at a distance of 10kpc for set 1 with $\beta = 1$ when the primary is in HG at the onset of RLOF. The black solid lines are for the results of SSP, which means a population without binary interaction, and the others are the contributions of BSs from different evolutionary channels. Note that the red solid lines are 5 times contributions of BSs from mass transfer (the thick ones) and from binary coalescence (the thin ones).

originate from mass transfer between AGB and MS stars, and have long-orbital periods in old clusters. However, it is still a puzzle in young open clusters – where does the extra He come from? It is possible that the merger models in Chen & Han (2008a) should be revised, e.g. the mass fraction of the primary mixed with the secondary is less than that assumed in that paper, but this fraction itself is now an open problem.

Many BSs observed in NGC 188, NGC 2682 and King 2 are in the regions from PBE, but we can obtain only one in each of the three clusters if we normalize BS numbers to N_2 (see Table 2). All of the three clusters are old open clusters and AML of low-mass binaries are much more important for BS formation than PBE in them. However, as shown in Table 2, although the number of BSs from AML may be as much as 4, AML also seems to be unable to explain the observed BS numbers in these three clusters. Meanwhile, AML should have no influence on BS formation in young open clusters, but we see from Table 2 that f is generally around 0.2 (much less than unity) in clusters younger than 1 Gyr, except for NGC 3114 ($f = 0.046$) and NGC 6475 ($f = 0.08$). The low BS specific frequency (less than 50 per cent in most cases) from our simulation for most clusters seems to support other channels producing BSs in addition

to PBE even in young open clusters. It is puzzling since PBE is expected to dominate BS formation in open clusters younger than 1 Gyr (see discussions in section 4.2).

4.2 Possible causes for the low specific frequency in the sample clusters

It is a serious problem that the BS specific frequency obtained in our simulations is much lower than that observed. Our first thought is to check the validity of the result. We examined the cases for $\log t = 9$ from Hurley’s rapid binary evolution code (Hurley, Tout & Pols 2002) based on the assumptions of simulation set 1 in this paper, and did find a higher value of f , i.e. $f = 0.3468$ for IC 166 and $f = 0.3796$ for NGC 2660. We checked and found that this is due to the different calculations of N_2 in the two codes. In Hurley’s code, a binary is treated as a single star, the SED of which comes from the contribution of two components, while in Han’s code, a binary is assumed to be two single stars, since the evolution of the primary after RLOF has not been followed. However, the values of f in Table 2 are still much less than that expected if we multiply by a factor of 2. Following are some discussions on this problem.

The value of f strongly depends on N_2 counted in clus-

Table 2. Parameters of Galactic open clusters with metallicity similar to that of the Sun ($Z = 0.02$). The bottom part shows the clusters which have no metallicity information available, but are rich in BSs from the new catalogue of AL07. We assumed solar metallicity ($Z = 0.02$) for these clusters when simulating. Columns (1)-(4) are cluster name, age [$\log(t/\text{yr})$], colour excess [$E(B - V)$] and distance modulus (the asterisks mean distance modulus corrected for absorption). Columns (5)-(6) are the metallicity (Z) and $[\text{Fe}/\text{H}]$ values, and columns (7) and (8) are N_2 (number of stars within 2 mag below the main sequence turnoff) and N_{BS} (numbers of BSs) in the sample clusters from observations (the data in brackets are from Xin et al.(2007)). Columns(9)-(11) show our simulation results from simulation set 1: $f_0 = N_{\text{bs}}^{\text{b}}/N_2^{\text{b}} \cdot N_2$, is the BS number expected from PBE. f'_0 is similar to f_0 but for that of AML, which is only shown for clusters older than 1Gyr. $f = f_0/N_{\text{bs}}$, is the ratio of the BS number expected from PBE to that of observed. As a comparison, we also show f from set 2 (which obviously differs from the other sets as presented in Fig.4) in brackets of column(11). The last column is the references for the data (note that the values of N_2 and N_{BS} in all clusters come from AL07): (1)AL07; (2)Vallenari et al. 2000; (3)Manteiga et al. 1995; (4)Bragaglia et al. 2000; (5)Claria et al. 2003; (6)Hebb et al. 2004; (7)van Leeuwen 1999; (8)Krusberg & Chaboyer 2006; (9)Kharchenko et al. 2005; (10)Loktin & Martkin 1994; (11)Dias et al. 2002; (12)Marshall et al. 2005; (13)Lapasset et al. 2000; (14) Vandenberg & Stetson 2004; (15)Eggen 1981; (16)Sarajedini et al. 2004; (17)Luck 1994; (18)Paunzen & Maitzen 2001; (19)Prosser et al. 1996; (20)Sagar et al. 2001; (21)Surendiranath et al. 1990; (22)Carraro & Patat 2001; (23)Balona & Laney 1995; (24)Ahumada 2005; (25)Andreuzzi et al. 2004.

Cluster Name (1)	$\log(t/\text{yr})$ (2)	$E(B - V)$ (3)	DM (4)	Z (5)	$[\text{Fe}/\text{H}]$ (6)	N_2 (7)	N_{BS} (8)	f_0 (9)	f'_0 (10)	f (11)	References
IC 166	9.00	0.80	15.65	0.02	0.00	120(110)	7(11)	1.36	-	0.194 (0.103)	1,2,3
IC 1311	8.95	0.45	14.10*	0.02	0.00	220(100)	12(7)	2.79	-	0.232 (0.100)	1,4
IC 2488	8.25	0.24	11.20	0.019	-0.02	30(10)	3(1)	0.58	-	0.192 (0.0511)	1,5
IC 4756	8.90	0.23	7.60*	0.022	0.04	80(55)	6(1)	1.07	-	0.178 (0.0690)	1,6
Melotte 111	8.60	0.00	4.77*	0.019	-0.03	10(10)	1(1)	0.16	-	0.160 (0.0452)	1,7
NGC 188	9.85	0.08	11.35	0.019	-0.01	185(170)	24(20)	0.72	3.78	0.0300 (0.0150)	1,8
NGC 1027	8.55	0.33	10.46	0.023	0.06	40(40)	0(2)	0.66	-	-	1,9,10
NGC 2287	8.39	0.03	9.30	0.022	0.04	30(30)	2(3)	0.52	-	0.258 (0.0705)	1,9,11
NGC 2301	8.31	0.03	9.76	0.023	0.06	20(15)	0(1)	0.35	-	-	1,9,11
NGC 2437	8.39	0.15	11.16	0.023	0.06	80(70)	7(5)	1.38	-	0.196 (0.0540)	1,9,11
NGC 2539	8.80	0.06	10.60	0.018	-0.04	100(20)	1(1)	1.37	-	1.371 (0.55)	1,12,13
NGC 2660	9.00	0.40	12.20*	0.02	0.00	150(110)	8(18)	1.70	-	0.213 (0.113)	1,4
NGC 2682	9.69	0.038	9.65	0.018	-0.04	175(200)	30(30)	0.72	2.31	0.0241 (0.013)	1,14
NGC 3532	8.54	0.04	8.59	0.019	-0.02	160(90)	5(9)	2.55	-	0.511 (0.169)	1,15,16
NGC 5316	8.19	0.27	11.26	0.019	-0.02	10(20)	0(4)	0.22	-	-	1,9,11
NGC 6067	8.11	0.32	11.17*	0.021	0.01	25(60)	3(7)	0.60	-	0.201 (0.035)	1,17
NGC 6281	8.51	0.15	8.93	0.02	0.00	20(25)	0(4)	0.32	-	-	1,9,11
NGC 6475	8.34	0.07	7.30	0.022	0.03	10(15)	2(2)	0.16	-	0.08 (0.0219)	1,11,19
NGC 6940	8.94	0.21	10.08*	0.021	0.01	90(130)	6(7)	1.16	-	0.193 (0.0796)	1,9,11
IC 1369	9.16	0.57	11.59*	0.02?	...	35(35)	6(6)	0.35	0.03	0.058 (0.0226)	1,10,11
King 2	9.78	0.31	13.80*	0.02?	...	250(250)	30(30)	0.97	4.01	0.032 (0.0159)	1,11
Melotte 105	8.40	0.52	11.80*	0.02?	...	80(25)	4(1)	1.37	-	0.341 (0.0923)	1,20
NGC 2818	8.70	0.22	12.90*	0.02?	...	45(45)	2(2)	0.70	-	0.347 (0.104)	1,21
NGC 3114	8.48	0.07	9.80*	0.02?	...	14(50)	5(5)	0.23	-	0.046 (0.0138)	1,22
NGC 3496	8.78	0.52	10.70*	0.02?	...	35(70)	1(4)	0.52	-	0.515 (0.129)	1,23
NGC 6416	8.78	0.25	10.12*	0.02?	...	50(35)	1(3)	0.74	-	0.735 (0.185)	1,9
NGC 6939	9.11	0.34	11.30*	0.02?	...	180(80)	5(4)	1.77	0.06	0.354 (0.161)	1,25

ters – a large N_2 leads to a higher f from eq(9), but for some clusters the observed values of N_2 are significantly different from various authors. For comparison, we show the values of N_2 and N_{BS} from Xin et al. (2007)(Xin07) in Table 2. We see that, for NGC 2539, the value of N_2 of AL07 is 5 times that of Xin07, leading to a factor of 5 difference of f . The value of N_2 from observation may be relevant to the cluster age and the distance modulus. For instance, in a distant cluster, stars are more difficult to detect, resulting in a smaller N_2 , and thus a smaller f . Also with increasing age, stars within 2 mag below the main-sequence turnoff become less massive and more difficult to detect, leading to a smaller f as well. Fig. 13 shows f varying with age and distance modulus for the sample clusters with known metallicity. However, we have not found correlations between f and the cluster

age when $\log t \leq 9$ or between f and the distance modulus. When $\log t > 9$, the value of f sharply decreases due to the decrease of N_{BS}^{b} and the increase of N_2^{b} (see section 3.2). Two clusters, NGC 2539 and NGC 3532, have f obviously larger than that for the others, due to the large N_2 from AL07. If we adopt the results of Xin07, f in these two clusters is much smaller and is similar to that in the other clusters.

From section 3.2 we know that the specific frequency of BSs depends heavily on the age. Thus, the precision of age determination also has effect on f , but the cluster age is very uncertain from observations. For instance, the age of NGC 2682 ranges from 3 (Bonatto & Bica 2003) to 6Gyr (Janes & Phelps 1994), which leads f to change from 0.0312 to 0.0231, about a factor of 1.35 difference.

Another possibility for the low f in our simulations is

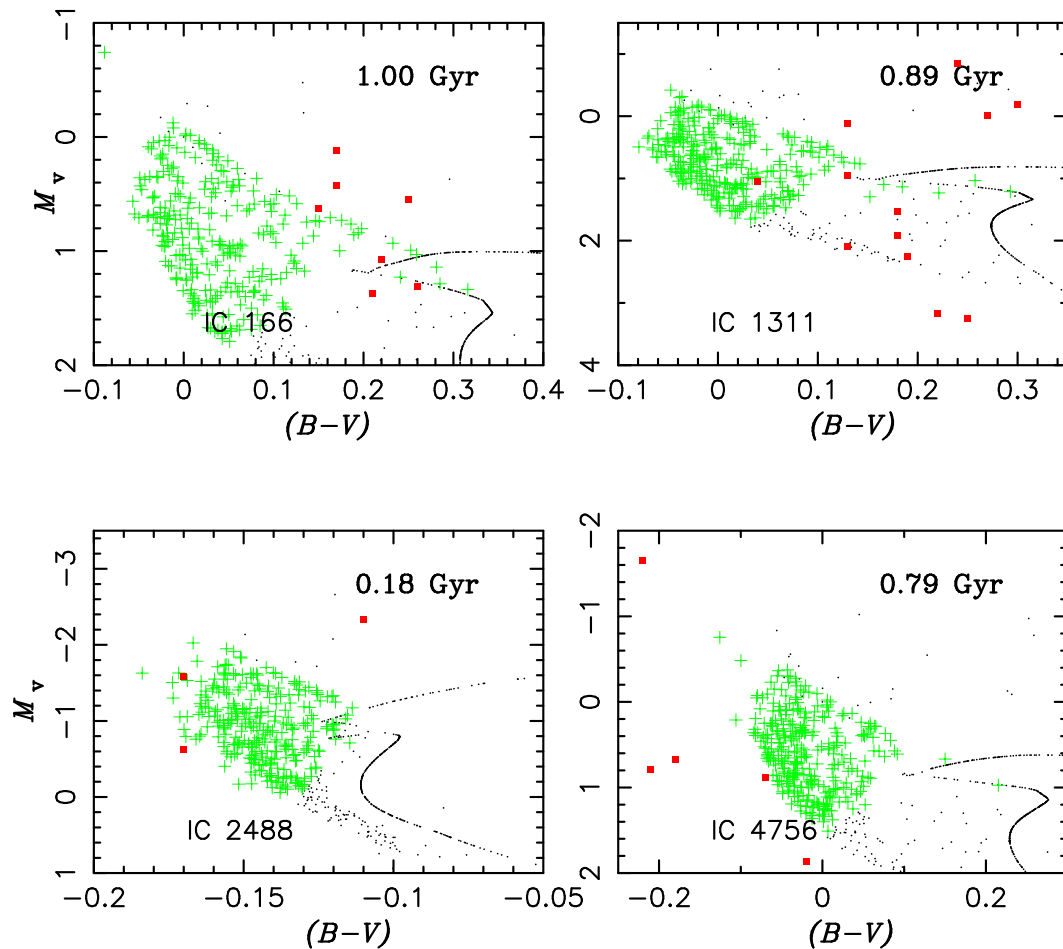


Figure 6. Colour-magnitude diagram for IC 166, IC 1311, IC 2488 and IC 4756. The crosses and squares are BSs from PBE and AL07, respectively. The dots are for all other stars in the cluster from our simulation.

that the adopted Monte Carlo simulation parameters (e.g. initial mass function) are different from those in the clusters. The Monte Carlo simulation parameters in this paper are for field stars and it is very likely that these parameters are different in clusters. For instance, the initial mass function is still an open problem and recent studies show that it might be quite different between disk stars and halo stars in the Galaxy (Pols et al. 2008). In addition, we know that low-mass stars are located in the extended region of the halo in old open clusters due to equipartition of energy. These objects are then likely to increase their velocities to be beyond the escape velocities of the host clusters and become field stars. Thus, the number of low-mass stars (less than $1M_{\odot}$) in old open clusters is much less than that expected from the IMF of the field stars. Moreover, both the binary frequency and the distribution of initial orbital periods of a population are important for BS production, and they are related to star formation history and environment of a cluster. Thus, they might be different even among open clusters.

Finally, the low f in our simulations might indicate other channels (e.g. a more recent era of star formation and dynamical interaction, see a review of Stryker 1993) to produce BSs in open clusters in addition to PBE and AML. Figure 13 shows that f in some clusters is lower than that

in the others. Thus, we cannot rule out other channels in these clusters, although we can multiply by a factor to increase f due to the causes above.

Discussions on binaries with a hot WD and a low-mass main-sequence star. What do these systems look like? Since the luminosity of a hot WD is much higher than that of main-sequence stars, it seems very likely that these systems are in the BS region. If so, we lose BSs like this in our simulations as we have not considered the contribution of the primaries after RLOF (initially hot WDs) to the SED. However, we should bear in mind that a hot WD mainly radiates in UV or far-UV, completely different from that of a low-mass main-sequence star. For example, a $0.57M_{\odot}$ CO WD is about 130000 K at 0.1Myr after its formation according to eq(90) in the paper of Hurley, Pols & Tout(2002). If we assume the WD to be a black body, the peak wavelength of its radiation is about 227\AA , and the flux at the peak wavelength is $f_{\lambda=227\text{\AA}} = 1.5 \times 10^{30} \text{ergs}^{-1}$, while f_{λ} is only about a few $10^{26} \text{erg.s}^{-1}$ at U,B and V bands. As the WD cools, the peak wavelength increases, but f_{λ}^{max} decreases. So the contributions of WDs in U, B and V bands are always much less than those of low-mass main-sequence stars, indicating that it is impossible that binaries with a hot WD and a low-mass main-sequence star look like BSs in the diagram of V versus B-V of a cluster. As a test, we examined the case of

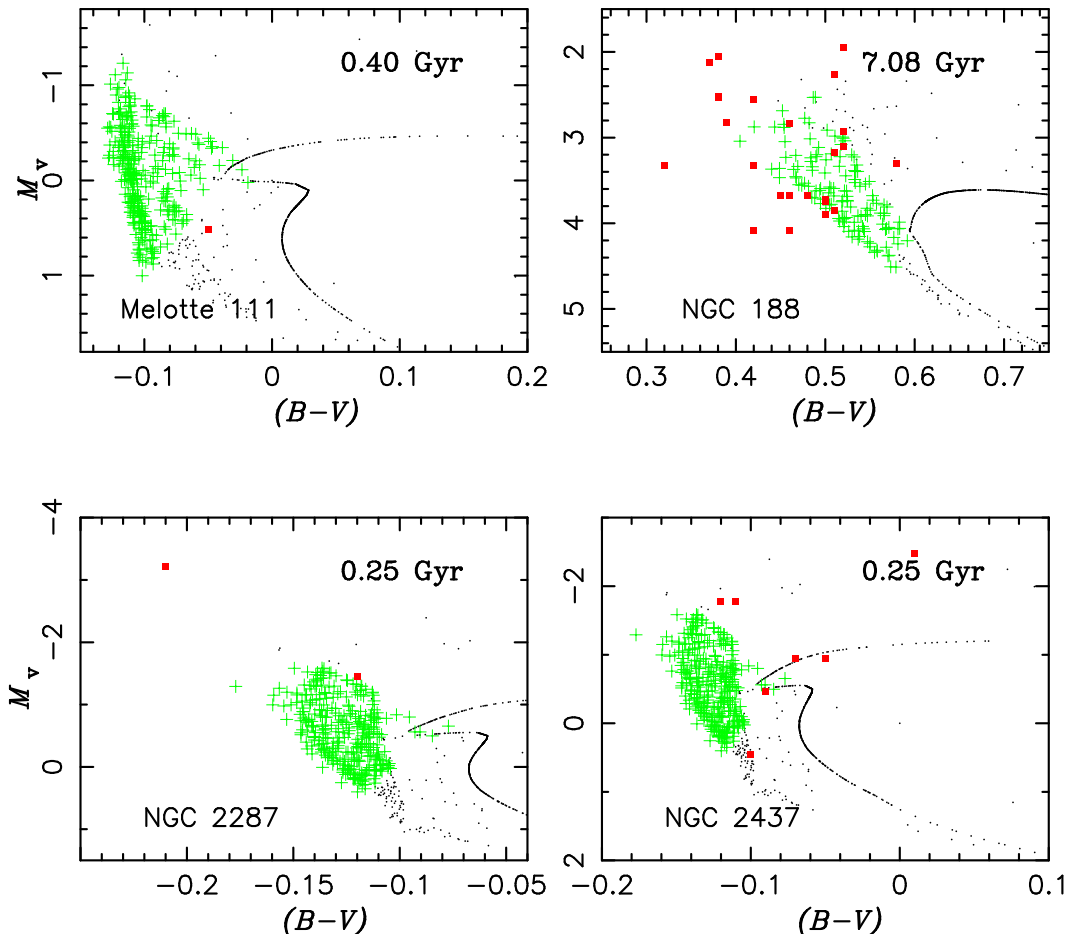


Figure 7. Similar to 6, but for Melotte 111, NGC 188, NGC 2287 and NGC 2437.

$t = 9.44$ Gyr, where both of two components of a binary are included (the primaries are WDs after RLOF), and found that all BSs obtained in this calculation are characterized by the main-sequence components, not the WDs.

5 SUMMARY

We systematically studied the BSs originating from primordial binary evolution (PBE) via a binary population synthesis approach, and examined their contribution to the integrated spectral energy of the host clusters. The study shows the following results: (a) PBE may produce BSs at any given age and BSs from it are located within 2.5 mag of the turnoff of the host cluster. (b) In UV and blue bands, BSs from PBE contribute the most energy for a population between 0.3 and 2.0 Gyr, and have a contribution similar to that of SSP between 2 and 4 Gyr. AML becomes more and more important for BS production with time, and its importance exceeds that from PBE in a population older than 3 Gyr. (c) BSs from PBE have an obvious scatter on the main sequence with decreasing mass (BS from AML also show this feature as shown in Fig.11 of Chen & Han 2008a) for populations between 0.4 and 1.5 Gyr. The scatter of BSs near the turnoff has been found in several open clusters. (d) Binary coalescence from contact binaries (*Channel II* in section 2.1)

is very sensitive to cluster ages, but BSs from it have relatively high mass. Thus, once *Channel II* works in a cluster, BSs from it become more important than those from other channels to contribute to the ISED of the cluster. (e) The value of β significantly affects on the final results, e.g the specific frequency of blue stragglers decreasing with β , blue stragglers produced from a high value of β having higher masses, then contributing more to the ISEDs of the host clusters. For old open clusters, the assumption of $\beta = 1$ when the primary is in HG at the onset of mass transfer matches the observations better than that of $\beta = 0.5$ from the locations of BSs on the CMDs.

We know that BPS results are sensitive to the uncertainties of the initial parameters, especially the initial mass-ratio distribution. Meanwhile, dynamical instability criteria during RLOF will also affect the final outcomes. Different simulation sets in this paper show that these parameters have little influence on the features above except for the BS specific frequency.

The main influence on the BS specific frequency comes from the distribution of initial mass ratio. The difference between set 1 (constant) and set 2 (uncorrected) may be up to about an order of magnitude for populations younger than 1 Gyr. With increasing time, the effect from dynamical instability criteria becomes obvious (up to about 0.5 dex), since more and more binaries undergo mass transfer between

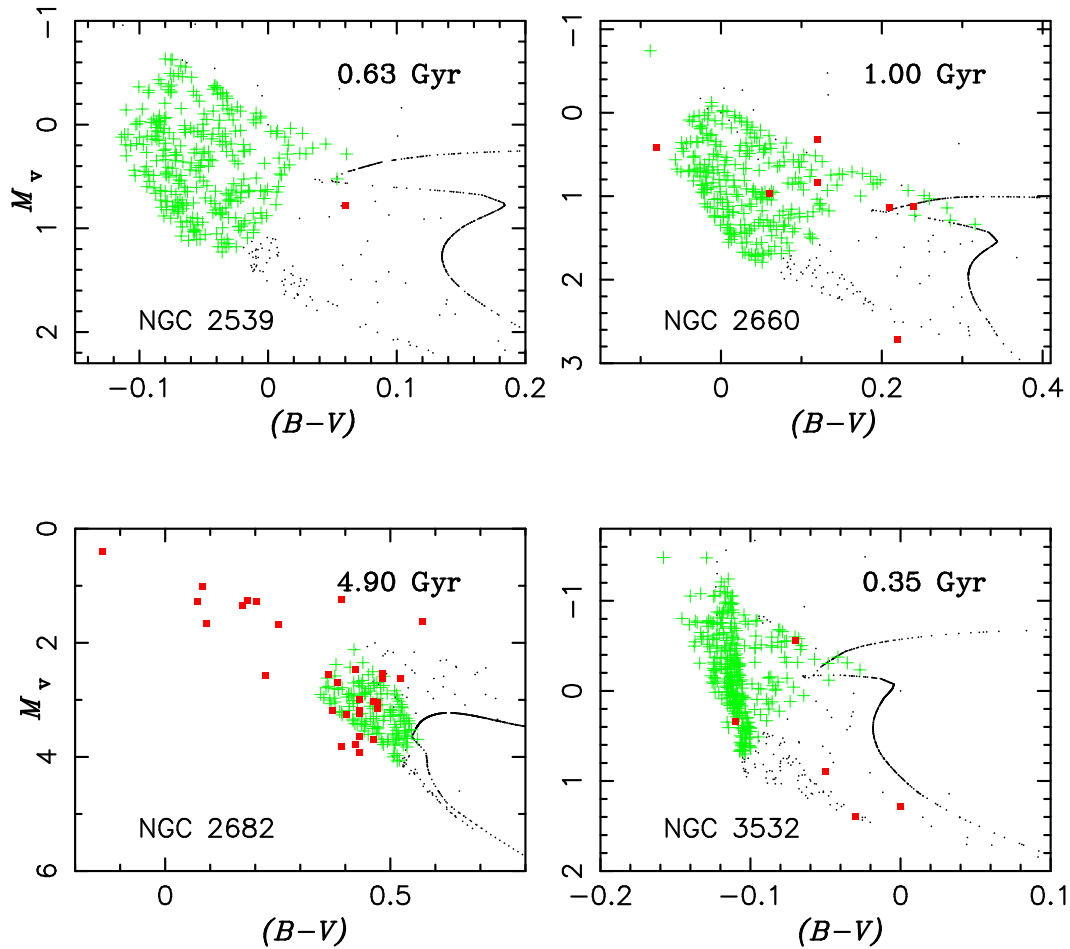


Figure 8. Similar to 6, but for NGC 2539, NGC 2660, NGC 2682 and NGC 3532.

giant stars and main-sequence ones. However, neither of the five sets in our simulations can produce enough BSs from PBE in comparison to observations in most Galactic open clusters, even in those younger than 1 Gyr. The ratio of the BS number expected from PBE to that of observed is only around 0.2 for most clusters we simulated. The role of AML in old open clusters is also less important than that of expected. It is puzzling and has been discussed in section 4.2.

6 ACKNOWLEDGMENTS

We are grateful to an anonymous referee for his/her valuable comments on our work and to Dr. Pokorny R. S. for his helpfulness improving the language of this paper. This work was in part supported by the Chinese National Science Foundation (Grant Nos. 10603013 and 10433030,10521001 and 2007CB815406), the Chinese Academy of Sciences (Grant No. 06YQ011001) and Yunnan National Science Foundation (Grant No. 08YJ041001).

REFERENCES

- Andreu G., Bragaglia A., Tosi M., Marconi G., 2004, MNRAS, 348, 297
- Andronov N., Pinsonneault M. H., Terndrup D. M., 2006, ApJ, 646, 1160
- Ahumada J., 2005, Astron. Nachr., 326, 3
- Ahumada J., Lapasset E., 2007, A&A, 463, 789
- Balona L. A., Laney C. D., 1995, MNRAS, 277, 250
- Bethe H. A., Brown G. E., Lee C. H., 2007, PhR, 442, 5
- Bilir S., Karatas Y., Demircan O., Eker Z., 2005, MNRAS, 357, 497
- Bonatto Ch., Bica E., 2003, A&A, 405, 525
- Bragaglia A., Tosi M., Marconi G., & Sandrelli S., 2000, in ASP Conf. Ser. 198, Stellar Clusters and Associations: Convection, Rotating and Dynamos, ed. R. Pallavicini, G. Micclla, & S. Sciortino (San Francisco: ASP), 51
- Carraro G., Patat F., 2001, 379, 136
- Chen X., Han Z., 2002, MNRAS, 335, 948
- Chen X., Han Z., 2003, MNRAS, 341, 662
- Chen X., Han Z., 2004, MNRAS, 355, 1182
- Chen X., Han Z., 2008a, MNRAS, 384, 1263
- Chen X., Han Z., 2008b, MNRAS, 387, 1416
- Claria J. J., Piatti A. E., Lapasset E., Mermilliod J.-C., 2003, A&A, 399, 543
- Dais W. S., Alessi B. S., Moitinho A., Lepine J. R. D., 2002, A&A, 389, 871
- Dalessandro E., Lanzoni B., Ferraro F. R., Rood R. T., Milone A., Piotto G., Valenti E., 2008, ApJ, 677, 1069
- Dewi J., Tauris T., 2000, A&A, 360, 1043
- Dryomova G. N., Svechnikov M. A., 2002, Ap, 45, 158
- Eggen O. J., 1981, ApJ, 246, 817

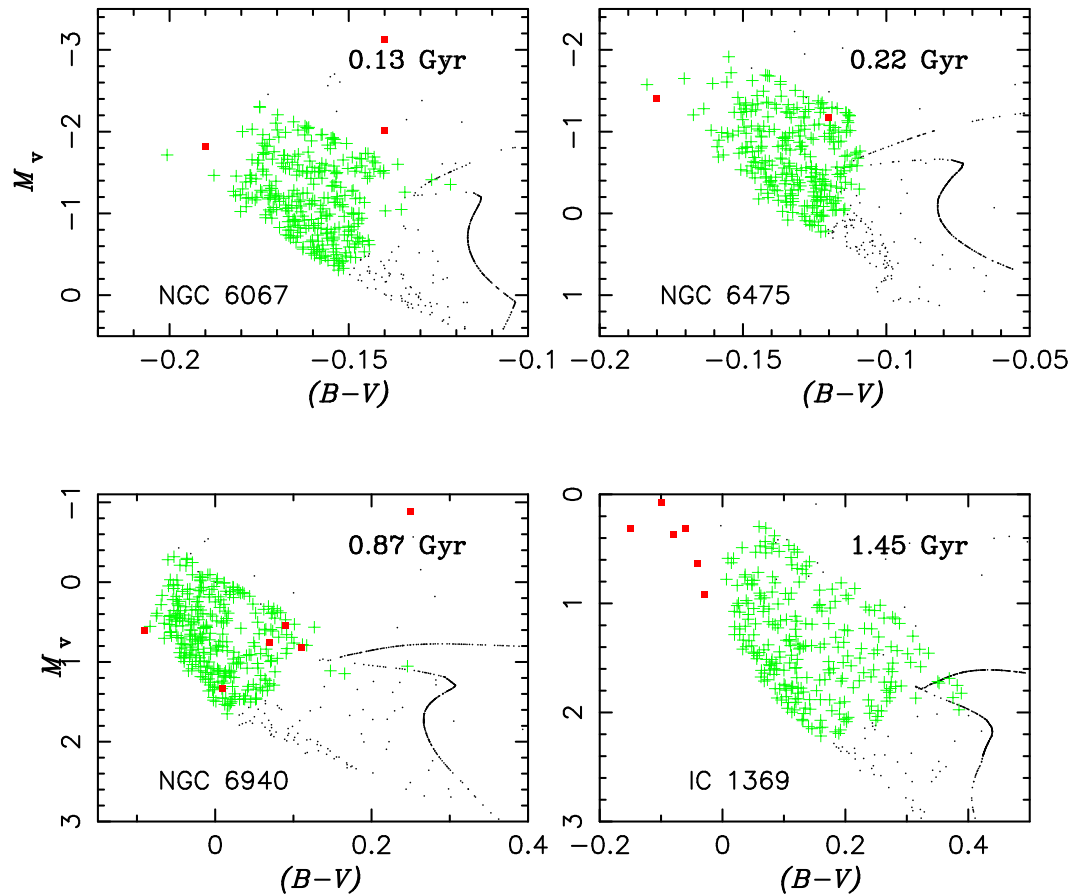


Figure 9. Similar to 6, but for NGC 6067, NGC 6475, NGC 6940 and IC 1369.

- Eggen O. J., Iben I. Jr., 1989, *AJ*, 97, 431
 Eggleton P.P., 1971, *MNRAS*, 151, 351
 Eggleton P.P., 1972, *MNRAS*, 156, 361
 Eggleton P.P., 1973, *MNRAS*, 163, 179
 Eggleton P. P., 1983, *ApJ*, 268, 368
 Eggleton P.P., 2000, *NewAR*, 44, 111
 Eggleton P.P., Fitchett M. J., Tout C. A., 1989, *ApJ*, 347, 998
 Glebbeek E., Pols O. R., Hurley J. R., 2008, arXiv0806.0863, accepted by *A&A*
 Han, Z., 1998, *MNRAS*, 296, 1019
 Han, Z.; Eggleton, P.P.; Podsiadlowski, Ph.; Tout C.A.; Webbink, R.F., 2001, *ASP Conf. Ser.*, 229, pp205-216
 Han Z., Podsiadlowski Ph., 2004, *MNRAS*, 350, 1301
 Han Z., Podsiadlowski Ph., Eggleton P.P., 1994, *MNRAS*, 270, 121
 Han Z., Podsiadlowski Ph., Eggleton P.P., 1995, *MNRAS*, 272, 800
 Han Z., Podsiadlowski Ph., Eggleton P.P., Tout C. A., 1995, *MNRAS*, 277, 1443
 Han Z., Podsiadlowski Ph., Lynas-Gray A. E., 2007, *MNRAS*, 380, 1098
 Han Z., Podsiadlowski Ph., Maxted P. F. L., Marsh T. R., Ivanova N., 2002, *MNRAS*, 336, 449
 Han Z., Podsiadlowski Ph., Maxted P. F. L., Marsh T. R., 2003, *MNRAS*, 341, 669
 Han Z., Tout C. A., Eggleton P. P., 2000, *MNRAS*, 319, 215
 Hebb L., Wyse R. F. G., & Gilmore G., 2004, *AJ*, 128, 2881
 Hjellming M. S., Webbink R. F., 1987, *ApJ*, 318, 794
 Hurley J. R., Pols O. R., Aarseth S. J., Tout C. A., 2005, *MNRAS*, 363, 293
 Hurley J. R., Tout C. A., Aarseth S. J., Pols O. R., 2001, *MNRAS*, 323, 630
 Hurley J. R., Tout C. A., Pols O. R., 2002, *MNRAS*, 329, 897
 Janes K. A., Phelps R. L., 1994, *AJ*, 108, 1773
 Kharchenko N. V., Piskunov A. E., Roeser S., Schibach E., Scholz R.-D., 2005, *A&A*, 438, 1163
 Kippenhahn R., Weigert A., 1967, *Z. Ap.*, 65, 251
 Krusberg Z. A. C., Chaboyer B., 2006, *AJ*, 131, 1565
 Langer N., Petrovic J., 2008, *IAUS*, 250, 167
 Lanzoni B., Dalessandro E., Perina S., Ferraro F. R., Rood R. T., Sollima A., 2007, *ApJ*, 670, 1065
 Lapasset E., Claria J. J., Mermilliod J.-C., 2000, *A&A*, 361, 945
 Lejeune T., Cuisinier F., Buesel R., 1997, *A&AS*, 125, 229
 Lejeune T., Cuisinier F., Buesel R., 1998, *A&AS*, 130, 65
 Li L., Han Z., Zhang F., 2005, *MNRAS*, 360, 272
 Loktin A. V., Matkin N. V., 1994, *Astron. Astrophys. Trans.*, 4, 153
 Luck R. E., 1994, *ApJS*, 91, 309
 Manteiga Outeira M., Acarreta Rodriguez J. R., Martinez Roger C., & Straniero O., 1995, in *IAU symp. 164, Stellar Populations*, ed. P. C., van der Kruit & g. Gilmore (Dordrecht: Kluwer), 377
 Marshall J. L., Burke C. J., DePoy D. L., Gould A., Kollmeier J. A., 2005, *AJ*, 130, 1916
 Mateo M., Harris H., Nemecek J., Olszewski E., 1990, *AJ*, 100, 469
 Mazeh T., Goldberg D., Duquenois A., Mayor M., 1992, *ApJ*, 401, 265
 Mc Crea W. H., 1964, *MNRAS*, 128, 147
 Miller G. E., Scalo J. M., 1979, *ApJS*, 41, 513
 Nelemans G., Verbunt F., Yungelson L.R. et al., 2000, *A&A*, 360,

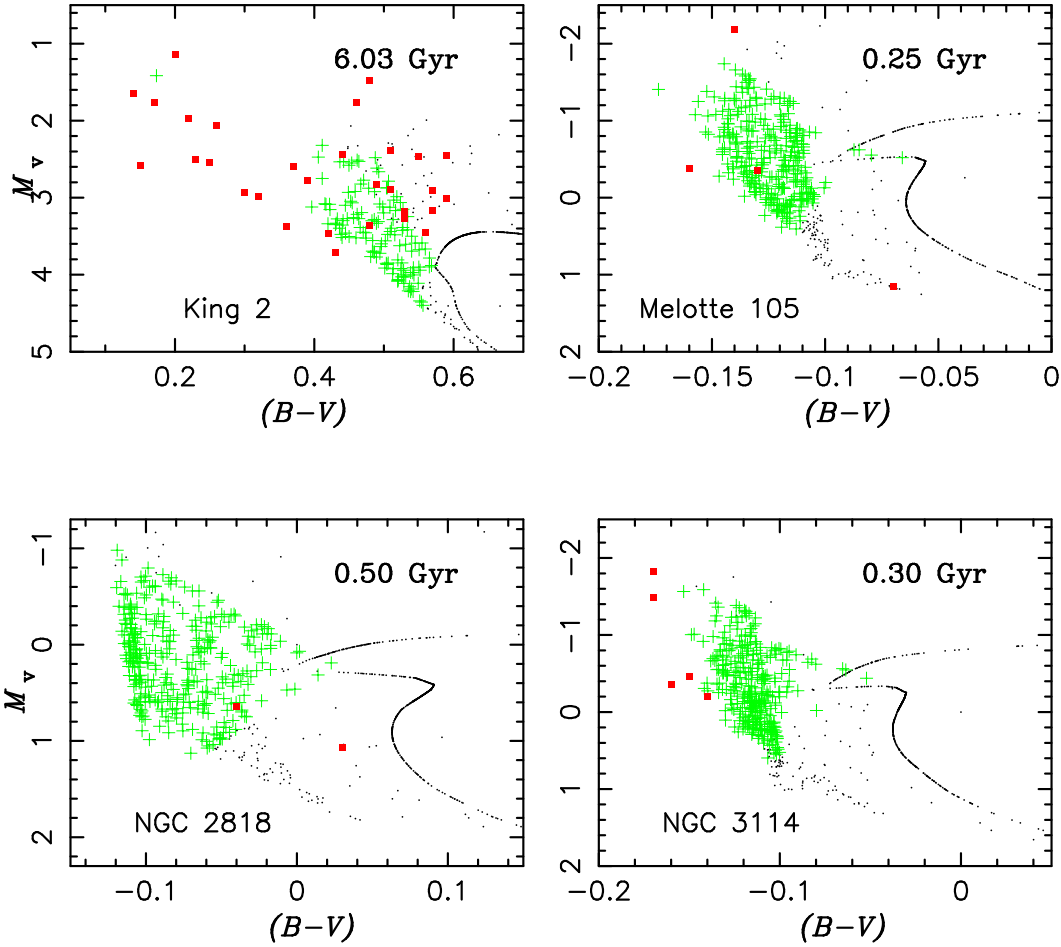


Figure 10. Similar to 6, but for King 2, Melotte 105, NGC 2818 and NGC 3114.

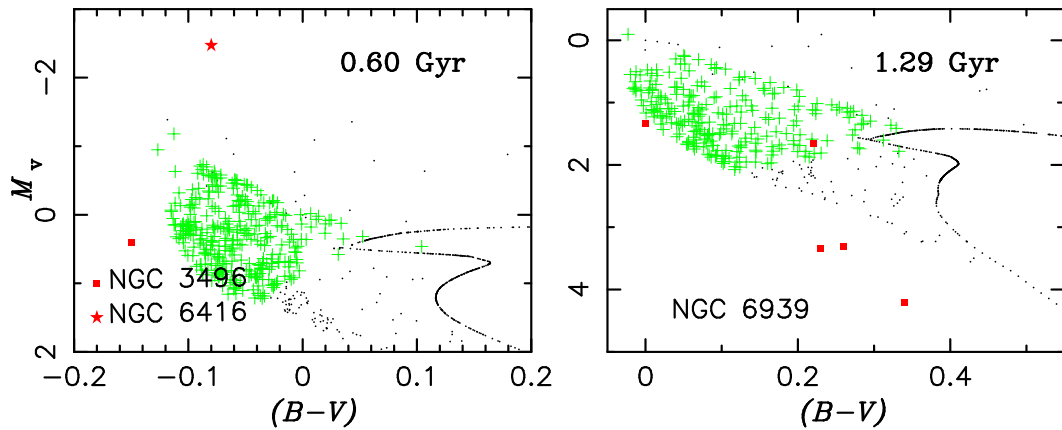


Figure 11. Similar to 6, but for NGC 3496, NGC 6416 and NGC 6939. Note that the results of NGC 3496 and NGC 6416 are in the same panel (in the left) since they have the same age, which results in the same CMD from our simulation.

1011
 Nelemans G., Tout C.A., 2005, MNRAS, 356, 753
 Paunzen E., Maitzen H. M., 2001, A&A, 373, 153
 Podsiadlowski Ph., Joss P. C., Hsu J. J. L., 1992, MNRAS, 391, 246
 Pols O. R., Izzard R. G., Lugaro M., de Mink S. E., 2008, IAUS, 252, 383
 Pols O. R., Marnus M., 1994, A&A, 288, 475
 Pols O.R., Schröder K.-P., Hurley J.R., Tout C.A., Eggleton P.P.,

1998, MNRAS, 298, 525
 Pols O.R., Tout C.A., Eggleton P.P., Han Z., 1995, MNRAS, 274, 964
 Prosser C. F., Randich S., Stauffer J. R., 1996, AJ, 112, 649
 Sagar R., Munari U., de Boer K. S., 2001, MNRAS, 327, 23
 Sandage A. R., 1953, AJ, 58, 61
 Sandquist E. L., Shetrone M. D., 2003, AJ, 125, 2173
 Sarajedini A., Brandt K., Grocholski A. J., Tiede G. P., 2004,

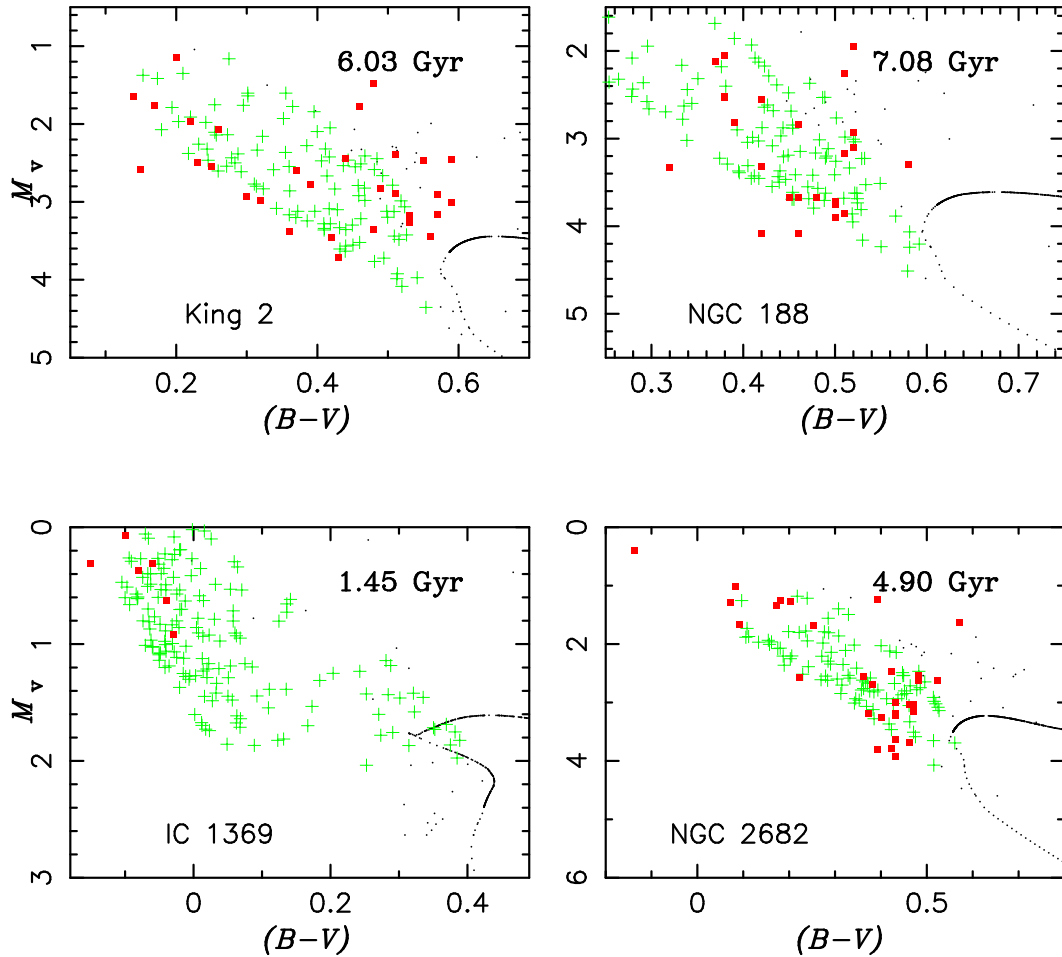


Figure 12. Similar to 6, but for King 2, NGC 188, IC 1369 and NGC 2682 and the mass transfer efficiency $\beta = 1$.

- AJ, 127, 991
 Soberman G. E., Phinney E. S., van den Heuvel E. P. J., 1997, A&A, 327, 620
 Sollima A., Lanzoni B., Beccari G., Ferraro F. R., Fusi Pecci F., 2008, A&A, 481, 701
 Stepien K., 2006, A&A, 56, 199
 Stryker L. L., 1993, PASP, 105, 1081
 Surendiranath R., Kameswara Raon N., Sagar R., Nathan J. S., Ghosh K. K., 1990, J. Astrophys. Astron., 11, 151
 Tian B., Deng L., Han Z., Zhang X., 2006, A&A, 455, 247
 Tutukov A. V., Fedorova A. V., 2007, ARep, 51, 291
 VandenBerg D. A., Stetson P.B., 2004, PASP, 116, 997
 van den Heuvel, E. P. J., 2006, Advances in Space Research, Volume 38, Issue 12, p. 2667-2672
 van Leeuwen F., 1999, in ASP. conf. Ser. 167, Harmonizing Cosmic Distance Scales in a Post-Hipparcos Era, ed. D. Egret & A. Heck (San Francisco: ASP), 52
 Vallenari A., Carraro G., Richichi A., 2000, A&A, 353, 147
 vant Veer F., 1994, Mem. S. A. It., 65, 105
 Webbink R. F., 1976, ApJ, 209, 829
 Webbink R. F., 2006, The Journal of the American Association of Variable Star Observers, Vol. 35, No. 1, p. 124-131
 Webbink R. F., 2007, arXiv0704.0280
 Xin Y., Deng L., 2005, ApJ, 619, 824
 Xin Y., Deng L., Han Z., 2007, ApJ, 660, 319

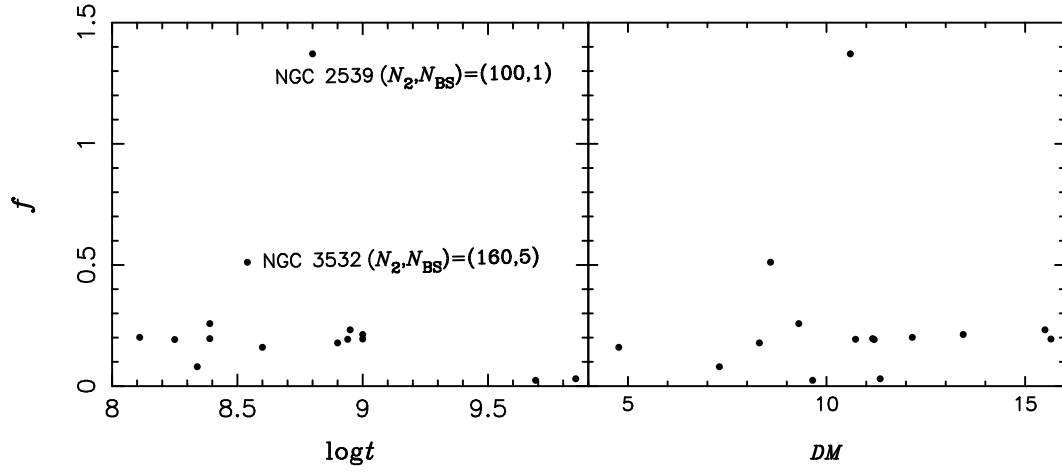


Figure 13. The ratio of the BS number expected from PBE to that of observed, f , versus the cluster age and distance modulus in the sample clusters with known metallicity. Two clusters, NGC 2539 and NGC 3532, have f obviously larger than that in the others. We show the values of N_2 and N_{BS} for the two clusters from AL07.